Transactions of the Materials Research Society of Japan 33[3] 583-586 (2008)

Nucleation, Expansion and Compression of Y_2O_3 nano-crystals: Crystallogenesis in Annealing Process of Metalorganic Decomposition Method

Masashi Ishii, Aiko Nakao* and Kenji Sakuai
National Institute for Materials Science (NIMS), 1-2-1 Sengen, Tsukuba, Ibaraki 305-0047 Japan
Fax: 81-29-860-4576, e-mail: ISHII.Masashi@nims.go.jp
* RIKEN, 2-1, Hirosawa, Wako, Saitama 351-0198, Japan
Fax: 81-48-462-4623, e-mail: anakao@riken.jp

Annealing process of Y_2O_3 thin film produced by metalorganic decomposition method was analyzed by x-ray reflectivity (XRR), x-ray diffraction (XRD), and atomic force microscopy. The annealing process was divided into two stages, stage I and stage II with respect to the annealing time. In the stage I, nuclei of Y_2O_3 nano-crystals were scatteringly formed in the Y-O precursor film just after the temperature rising. As the annealing progresses, expanding nano-crystals filled up the film and covered the surface smoothly, resulting in a clear XRR oscillation. From XRD analyses, volume-weighted average diameter of the nano-crystals to produce the smooth surface was estimated to be ~10 nm. In the following stage II, the Y_2O_3 nano-crystals did not expand any more; the crystals did not make a large domain by bunching. On the other hand, degenerative XRR oscillation in stage II revealed that stress at the grain boundary forces up the nano-crystals, resulting in rough interface and/or surface of Y_2O_3 thin film. Besides that, XRD peak was shifted to higher angle in this stage, indicating that the surface energy of the Y_2O_3 nano-crystals was so small that the crystal lattice was compressed without release of the internal energy.

Key words: x-ray reflectivity, x-ray diffraction, Y_2O_3 nano-crystals, surface roughness, compression of crystal lattice

1. INTRODUCTION

In recent years, interface chemical reactions are considered to be applicable for data storage [1-2]. The interface reactions produce a thin layer with a specific chemical composition different from the adjoining materials, resulting in huge modulation of electric and magnetic properties. Since the modulation is equivalent to switching of the states, it is applicable to durable data printing in media, post-formation of nano-structures in layered structures, and holographic memory [3]. For these data memorization and nano-architectonics, we are focusing on the oxidization-reduction at metal/oxide interfaces. At the metal/oxide interface, since the oxygen atoms can be translated between the metal and the oxide, the composition in atomic-layer level can be changed by a thermal- or electric-trigger [4]. Moreover, controllability and stability of the oxides are advantageous to the post-formation of nano-structures at buried interface. In previous studies, we found a metal/yttria (Y_2O_3) interface reaction at ultra-low temperature of ~100 °C [5]. The low reaction temperature does not modulate the bulk structures of metal and Y_2O_3, suggesting that the O translation is not diffusive and is limited within atomic-layer level at the interface. In fact, the interface reaction did not destroy the stacking structure and kept atomic-scale flatness on the surface.

Although the extraordinary low-temperature reaction is valuable for data writing in the memory devices, the reaction details have never been investigated. First of all, since Y_2O_3 used in our study is polycrystalline, the reaction would be sensitive to the grain size and shape. Therefore, the initial surface and interface before the reaction should be characterized.

X-ray reflectivity (XRR) measurements can non-destructively provide structural information of layered structure with high depth resolution < ~nm [6]. It is also quite sensitive to the surface and interface roughness. These potential abilities suggest the applicability of XRR measurement to evaluation of the thin films. On the other hand, considering the small gracing angle of ~mrad in XRR measurement and x-ray beam size of sub-mm, it is a macroscopic analysis observing very wide area. However the combination of another macroscopic analysis, x-ray diffraction (XRD) with XRR provides microscopic surface model. In this paper, we perform a combination analysis to characterize the microscopic Y_2O_3 surface before deposition of the metal for the interface formation. Finally, the surface model is corroborated by a local measurement, atomic force microscopy (AFM).

2. EXPERIMENTS

Y_2O_3 film with about 50 nm thick was formed on Si (100) wafer with a metalorganic decomposition method [7] (MOD method, Kojundo Chemical Laboratory Co., Ltd.). In the MOD method, a metalorganic solution (product name of Y-03) including Y and O elements were dropped on the Si wafer, and the droplet was spread over by a spin coater. Two-step coating on 1000 rpm (revolutions per minute) for 10 sec and following 3000 rpm for 40 sec was adopted. After 2 min drying at 120 °C, the coated sample was annealed at 550 °C to crystallize the coated Y-O precursor film. We analyzed

the annealing process by XRR, in-plane XRD and AFM. For the XRR and XRD measurements, we used RINT-ATX (Rigaku Corporation, UltraX18 and in-plane goniometer). AFM for evaluation of surface morphology was performed with SPM9500-J3 (Shimadzu Corporation).

3. RESULTS AND DISCUSSION

3.1 XRR and XRD analyses

Figure 1(a) indicates the annealing process of Y_2O_3 thin layer on Si substrate observed by the XRR measurement. The data is vertically displaced with increasing annealing time. As shown in this figure, XRR continuously changed with increasing annealing time; the XRR oscillation amplified abruptly at 30 min and after that it gradually lessened. Finally, the oscillation completely disappeared at the annealing time of 90 min. This result suggests that the Y_2O_3 annealing process is divided into two stages altering at ~30min. In this paper, we denote the stages as "Stage I" for shorter annealing time than 30 min and "Stage II" for longer than 30 min.

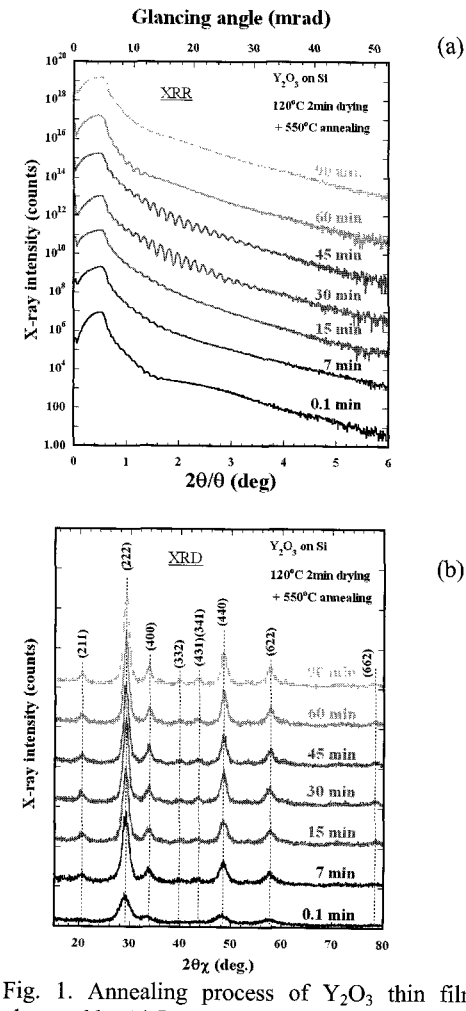

Fig. 1. Annealing process of Y_2O_3 thin film on Si observed by (a) XRR and (b) *in-plane* XRD.

Corresponding *in-plane* XRD shown in Fig. 1(b) is consistent with the two-stage model. In the XRD measurements, x-ray incidence angle θ was fixed at 0.35° and $2\theta\chi$ scanning was performed for probing x-ray diffractions from the Y_2O_3 thin film on the Si wafer. From the surface sensitive XRD measurement, we can discuss the crystallogenesis of the Y_2O_3 thin film.

As shown in Fig. 1(b), XRD results indicated formation of the Y_2O_3 polycrystalline independent of the annealing time and no prior crystal orientation was observed. As the Y_2O_3 thin film is annealed, the diffraction peaks from Y_2O_3 polycrystalline are gradually strengthened and do not buildup after 30 min any more, indicating that the crystallization is completed at 30min. From the comparison between Figs. 1(a) and (b), the crystallization process found in the peak strength of XRD is parallel with the stage I explained in XRR of Fig. 1(a).

For more quantitative evaluations of the XRD shown in Fig. 1 (b), we fitted the Y_2O_3 (222) diffraction peak at $2\theta_\chi \sim 29.2°$ with a Lorentzian function. Examples of the fitting are shown in Fig. 2. As shown in this figure, the Loretntzian function well reproduced the experimental diffraction peaks independent of the annealing time from 0.1 min (open circles) to 90 min (closed circles). Therefore, in the following discussions, we deal with the parameters obtained by the fitting for precise characterization of the peak profile.

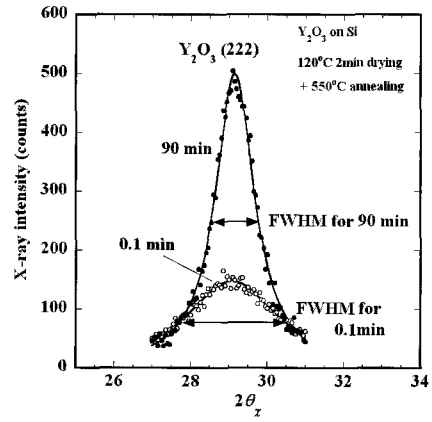

Fig. 2. Y_2O_3 (222) XRD peaks fitted with Lorentzian function.

From the full width at the half maximum (FWHM) of the diffraction peak, we can estimated size of the Y_2O_3 crystal grains D with Scherrer's equation [8-9],

$$D = \frac{K\lambda}{B\cos\theta}, \qquad (1)$$

where λ is wavelength of x-ray, B is the FWHM of the diffraction peak, θ is Bragg angle of the peak, and K is Scherrer constant. λ in this study was 1.5418 Å of Cu Kα. We applied the fitting parameters of Y_2O_3 (222) diffraction peak to eq. (1). In actual system, B is given by $B_{fit} - b$, where B_{fit} can be obtained from the Lorentzian fitting and b is that of XRD peak for a prevailing material with sufficiently large grains. In this study, b is estimated from a diffraction peak of a commercially provided Si single crystal wafer. By the substitution of $B_{fit} - b$ for B, the system parameters dependent on the apparatus are convoluted into eq. (1). K depends on the assuming shape and so we adopt $8/3\pi$ for spherical grains [10]. In this case, D gives the

volume-weighted average diameter expressed by

$$D = \frac{V_1 d_1 + V_2 d_2 + \cdots + V_i d_i}{V_1 + V_2 + \cdots + V_i}, \quad (2)$$

where V_i and d_i are the volume and diameter of a grain i. Note that the D values discussed in this paper are based on the assumptive shape of the spherical grain.

The volume-weighted average diameters estimated from eq. (1) applied to the Y_2O_3 (222) diffraction peak are summarized in Fig. 3. As shown in this figure, the Y-O precursor by the MOD method forms nucli of Y_2O_3 crystal with a few nm diameter right after the temperature rising. The nano-crystals expand with increasing annealing time, and its diameter saturated at ~10 nm after the annealing for 30 min. The saturation of D for the sufficiently long annealing time indicates that the nano-crystals do not bunch up to make a large domain.

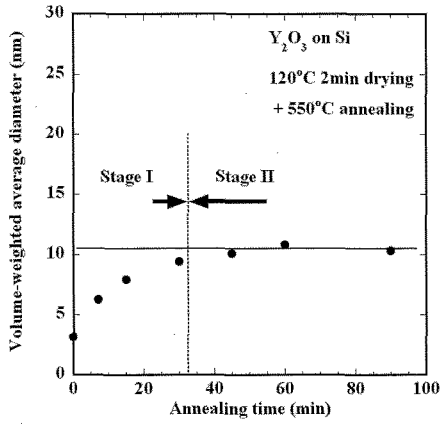

Fig. 3 Volume-weighted average diameter of Y_2O_3 nano-crystals vs. annealing time.

Remember that XRR in Fig. 1(a) provides the two-stage annealing process different from XRD in Fig. 3. As discussed below, the combination analysis of macroscopic XRR and XRD measurements provides a microscopic model on the Y_2O_3 surface during the annealing. In the following discussions, the layered structure with a flat surface and an abrupt interface providing clear XRR oscillation is referred as the *well-defined structure*.

In the stage I of the annealing process, although XRR indicated that the well-defined structure of Y_2O_3/Si was established just on 30 min, XRD showed that Y_2O_3 began to crystallize right after the temperature rising at 550 °C. These findings indicate that the Y_2O_3 crystallization does not directly correlate with the well-defined structure. However, the annealing processes for formation of the well-defined structure and the crystallization of the nano-crystals can be consistently explained as follows. At the early stage of the stage I, the nuclei of Y_2O_3 nano-crystals are scatteringly and independently formed in the Y-O precursor film prepared by the MOD method. The scattering formation of Y_2O_3 nano-crystals is not effective in magnifying the XRR oscillation because of dominant covering by a soft precursor at the interface. On the other hand, the nano-crystals can be detected with XRD surely. As the annealing progresses, the expanding nano-crystals fill up the film and cover the surface and interface smoothly, resulting in the well-defined structure just on 30 min. Then, the XRR oscillation is strengthened by the well-defined structure at last. On the other hand, XRD provides the filling up process gradually.

In the stage II, the size of the Y_2O_3 nano-crystals evaluated from FWHM of the XRD peak was not changed by the annealing longer than 30 min (see Fig. 3). The fact suggests that the expanding nano-crystals without bunching yield huge stress at the boundary. The stress lifts out the nano-crystals from the surface, resulting in rough interface and/or surface of Y_2O_3 thin film. Consequently, the surface/interface roughening vanish the XRR oscillation for the long time annealing such as 90 min (Fig. 1(a)).

This surface/interface roughening model of the stage II indicates low surface energy of the Y_2O_3 nano-crystals. Although the stress can be released by the lift out of the nano-crystals on the Y_2O_3 surface, it is accumulated in the film. Therefore, internal energy of the nano-crystals increases. It can be confirmed by lattice distortion in the crystals. Figure 4 shows the $2\theta_\chi$ diffraction angle of the Y_2O_3 (222) peak versus the annealing time. The diffraction angle in this figure was evaluated from the fitting with the Lorentzian function. In the stage I, the $2\theta_\chi$ angle is constant at ~29.132°. On the other hand, in the stage II, the $2\theta_\chi$ angle increases with increasing annealing time. Since the lattice constant d is correlated with θ_χ by $\lambda/2\sin\theta_\chi$, the increase of $2\theta_\chi$ in the stage II means decrease of d, i.e., compression of the Y_2O_3 nano-crystals. The expanding Y_2O_3 nano-crystals strongly compress themselves, but the stress cannot be released by bunching to make large domains.

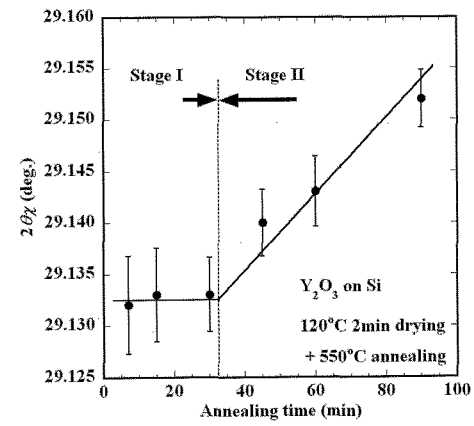

Fig. 4 $2\theta_\chi$ of Y_2O_3 (222) diffraction peak as a function of annealing time.

3.2 AFM analyses

Surface morphology of the Y_2O_3 thin film observed by AFM approves the annealing model proposed in the XRR and XRD analyses in 3.1. Figure 5 shows surface roughness with respect to the annealing time. As shown in this figure, the shorter annealing correspondent to the stage I flattens the Y_2O_3 surface from ~1.5 nm to ~0.5 nm in rms. (root mean square). It is consistent with the filling up process of the expanding Y_2O_3 nano-crystals

and densely covering the surface and interface found in x-ray analyses. On the other hand, the longer annealing correspondent to the stage II roughens the Y_2O_3 surface in AFM image. As discussed in the section 3.1, it can be understood by to the force up process of the rushing nano-crystals.

The nano-crystals roughening the surface can be seen in the actual image. Figure 6 shows AFM image for (a) 30 min and (b) 90 min annealing times. The vertical and horizontal scales in these images are same. After 30 min annealing shown in Fig. 6(a), moderate bumps with ~nm height cover the surface. On the other hand, it can be seen that many grains with sharp edge are lifted out for 90 min annealing as indicated in Fig. 6(b).

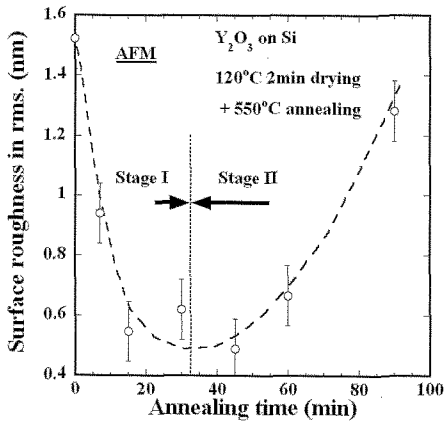

Fig. 5 Surface roughness estimated from AFM vs. annealing time

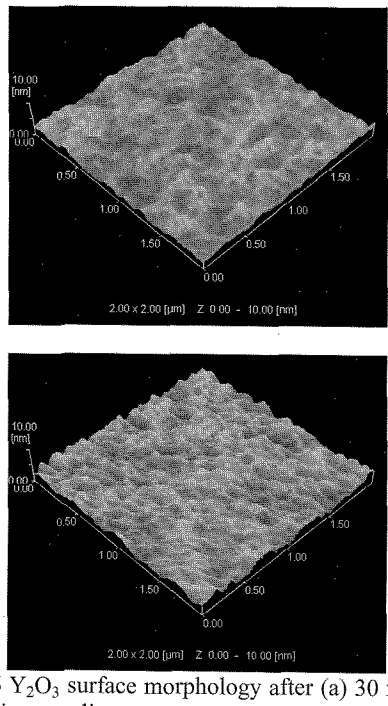

(a)

(b)

Fig.6 Y_2O_3 surface morphology after (a) 30 min and (b) 90 min annealing.

Recently, we found a low temperature reaction of metal/Y_2O_3 systems [5]. The reaction can be observed for the Y_2O_3 thin film prepared by the MOD method with 30 min annealing. From the analyses in this paper, the original Y_2O_3 thin film before the metal deposition is characterized as follows. The film is polycrystalline constructed from the nano-crystals with a volume-weighted average diameter of ~10 nm. The crystals cover the surface and interface densely, but the stress at the boundary of the nano-crystals is negligible, i.e., no excessive compression in the crystals. The surface of the Y_2O_3 film has atomically flatness of ~0.5 nm in rms. The low temperature reaction can be proved from the change of these properties.

4. SUMMARY

The crystallogenesis of Y_2O_3 nano-crystals from a Y-O precursor prepared by a metalorganic decomposition (MOD) method was discussed by a combination analysis of x-ray reflectivity (XRR) with x-ray diffraction (XRD). In the early stage of 550 °C annealing of MOD film, nuclei of Y_2O_3 nano-crystals were scatteringly formed in the precursor film. The nuclei grew up by the annealing, and the expanding nano-crystals covered the surface smoothly. Since the precursor film could not make the smooth surface and interface, clear XRR oscillation was observed just on time for the covering by the nano-crystals. After the covering, the nano-crystals were not expand any more, but strongly compressed by their squash. Moreover, the excessive compression lifted up the nano-crystals outside of the film, resulting in surface roughness. These findings indicate that the surface energy of the Y_2O_3 nano-crystals is so small that the crystals compress themselves but do not bunch up for the stress release.

This work is partly supported by KAKENHI, Grant-in-Aid for Scientific Research (C) (19560029) from The Ministry of Education, Culture, Sports, Science and Technology (MEXT), Japan.

REFERENCES

[1] K. Terabe, T. Hasegawa, T. Nakayama, and M. Aono, Nature, 433, 47-50 (2005).
[2] A. Asamitsu, Y. Tomioka, H. Kuwahara, and Y. Tokura, Nature, 388, 50-52 (1997).
[3] T. Morikawa, T. Nakajima, and K. Sakurai, 23, 405-406 (1973).
[4] M. Ishii, A. Nakao, and K. Sakurai, MRS 2007 Fall Proceedings, 1065E (to be published).
[5] M. Ishii, A. Nakao, and K. Sakurai, J. Phys.: Conf. Ser., 83, 012014 (2007).
[6] K. Sakurai, and A. Iida, Jpn. J. Appl. Phys., 31, L113-115 (1992).
[7] H. Fukuda, S. Maeda, K. M. A. Salam, and S. Nomura, 41, 6912-6915 (2002).
[8] P. Scherrer, Nachr. Ges. Wiss. Göttingen, 26 September, p.98-100 (1918).
[9] S. Calvin, S. X. Luo, C. Caragianis-Broadbridge, J. K. McGuinness, E. Anderson, A. Lehman, K. H. Wee, S. A. Morrison, and L. K. Kurihara, Appl. Phys. Lett. 87, 233102 (2005).
[10] T. Ida, S. Shimazaki, H. Hibino, and H. Toraya, J. Appl. Cryst., 36, 1107-1115 (2003).

(Recieved December 10, 2007 ; Accepted February 27, 2008)